

Original Article

Is Cochlear Length Related to Congenital Sensorineural Hearing Loss: Preliminary Data

Mehmet Bilgin Eser , Başak Atalay , Mahmut Tayyar Kalcioğlu 

Department of Radiology, Istanbul Medeniyet University School of Medicine, Istanbul, Turkey (MBE, BA)

Department of Otorhinolaryngology & Head and Neck Surgery, Istanbul Medeniyet University School of Medicine, İstanbul, Turkey (MTK)

ORCID IDs of the authors: M.B.E. 0000-0003-2490-9449; B.A. 0000-0003-3318-3555; M.T.K. 0000-0002-6803-5467.

Cite this article as: Eser MB, Atalay B, Kalcioğlu MT. A Preliminary Data: Is Cochlear Length Related to Congenital Sensorineural Hearing Loss? J Int Adv Otol 2021; 17(1): 1-8

OBJECTIVES: This study used the data from patients with congenital sensorineural hearing loss (CSNHL) and those with normal hearing to measure and compare the length of the cochlea with high-resolution computed tomography (HRCT).**MATERIALS and METHODS:** HRCT images of patients who were diagnosed with CSNHL and were candidates for cochlear implantation were evaluated retrospectively. Sixty-three ears of 33 patients were included in the study. The control group comprised 66 ears of 33 individuals. The measurements were conducted by an experienced radiologist, using three-dimensional curved multiplanar reconstruction. All the measurements were performed thrice, and the average was calculated.**RESULTS:** The data were distributed normally. The lengths of the cochlear components for the CSNHL and control groups were as follows: basal turn 21.66 ± 1.01 (21.30-22.02) and 22.57 ± 0.68 (22.32-22.81) mm, middle turn 11.58 ± 0.69 (11.34-11.83) and 12.39 ± 0.46 (12.23-12.56) mm, and apical turn 6.45 ± 0.92 (6.12-6.77) and 7.12 ± 0.65 (6.89-7.35) mm, respectively. The mean cochlear lateral wall (LW) length was significantly shorter in the CSNHL patients [39.71 ± 1.32 (39.25-40.18) mm] than in the controls [42.09 ± 1.17 (41.67-42.51) mm], ($p < 0.001$). The intra-rater reliability was 0.878 (confidence interval 95%: 0.841-0.908 $p < 0.001$). The cut-off value was 40.81 mm (sensitivity: 0.91, specificity: 0.94, and accuracy: 0.90).**CONCLUSION:** There were microanatomic dissimilarities between the length of the cochlea in subjects from the CSNHL group and those from the control group.**KEYWORDS:** Cochlear hearing loss, helical CT, computer-assisted three-dimensional imaging, cochlear implantation, sensorineural hearing loss

INTRODUCTION

Measurement of the length of the organ of Corti (OC) and lateral wall (LW) has been performed using histological-radiological and direct-indirect methods^[1]. Many studies have also used different spiral equations^[2,3]. Individuals included in previous histological studies were randomly selected from the population, and their hearing status is unknown.^[4-9] Radiological measurement methods were first used with direct radiography^[10,11]. Thereafter, computed tomography (CT), thin-section high resolution computed tomography (HRCT), cone beam computerized tomography (CBCT), and micro-CT methods have been used recently^[6,12-16]. Of these, only HRCT and CBCT can be used for in-vivo evaluation^[13-16]. However, these two methods offer insufficient resolution for the imaging of the OC. Therefore, indirect measurement methods are now used more frequently. One of the most regularly used indirect methods for measuring the length of the OC is the measurement or calculation of LW length^[2,3,13-16].

Recently, some research has focused on in-vitro micro-CT for imaging and measuring the OC^[6,7]. The results of these studies are similar to those obtained via the histological direct measurement method^[8,9].

Studies on LW measurement have been mainly performed on ears with an unknown history of hearing status^[4-6,13-15]. Purcell et al.^[17] and Shim et al.^[18] measured and compared the cochlear dimensions of individuals with congenital sensorineural hearing loss (CSNHL) and controls. However, to our knowledge, no study has compared the two groups with the measurement of the length

This study was presented at the 5th Congress of the Confederation of European Otorhinolaryngology-Head and Neck Surgery, June 29-July 3, 2019, Brussels, Belgium and 7th National Congress of Otolaryngology and Neurotology, April 4-7, 2019, Antalya, Turkey.

Corresponding Address: Mahmut Tayyar Kalcioğlu E-mail: mtkalcioğlu@hotmail.com

Submitted: 30.10.2019 • **Revision Received:** 16.12.2019 • **Accepted:** 23.12.2019 • **Available Online Date:** 09.03.2020

Available online at www.advancedotology.org



Content of this journal is licensed under a
Creative Commons Attribution-NonCommercial
4.0 International License.

of the cochlea from the round window to the apex. Measurement of the OC length is vital for reducing the risk of damage during cochlear implantation surgery and can improve the success rate in terms of postoperative hearing and preservation of residual hearing [4, 5, 19-24].

According to the literature, 20% of CSNHL patients have gross anomalies that can be diagnosed with imaging and most of these anomalies are genetically influenced. In up to 80% of patients with CSNHL, the cochlea and other inner ear structures appear normal [17, 18, 25]. We focused on the cochlear microanatomy of non-syndromic CSNHL patients with normal cochlea as per the Sennaroglu classification [25]. Although the appearance of the cochlea in idiopathic CSNHL patients is similar to that in the healthy group, there may be differences in their microanatomy.

This study aimed to use HRCT to investigate the difference in the cochlea length of patients with CSNHL and those with normal hearing. We measured and compared the length of the LW on imaging using temporal bone HRCT in both CSNHL patients and controls.

MATERIALS AND METHODS

This study was approved by the Istanbul Medeniyet University, Göztepe Training and Research Hospital Ethics Committee for Clinical Studies (17 May 2018, 2018/0177).

Materials

The patient group consisted of CSNHL patients who were detected in the newborn screening by using automatic auditory evoked brainstem responses (ABR) with 35 dB HL click stimuli. Patients who had hearing loss were evaluated with diagnostic audiological tests, and otoscopic examinations were performed. After these tests, if the child was diagnosed with hearing loss, binaural hearing aids were used. For children with profound sensorineural hearing loss who could not benefit from hearing aids, cochlear implant surgery was recommended and performed when the child was about one year old. For these children, preoperative HRCT images were obtained before the cochlear implantation (CI) surgery in our university hospital. This study included CSNHL patients' HRCT images undertaken between January 2013 to September 2019. The cochlea of this group had 2½ or 2¾ turns and had no anomalies according to the Sennaroglu classification [25]. Patients diagnosed with congenital infectious diseases that could have caused CSNHL, such as *Toxoplasma gondii*, rubella virus infection, cytomegalovirus infection, and herpes simplex virus infection, along with syndromic patients were excluded. The detailed inclusion and exclusion criteria for the study population are presented in Figure 1. Archived images were available for 33 of 39 patients who met the inclusion criteria. Total 30 right and 33 left ears were included in the patient group. Since CI was performed for the right ear of three patients previously, the right ear images had artifacts and were excluded from the study. Thus, it

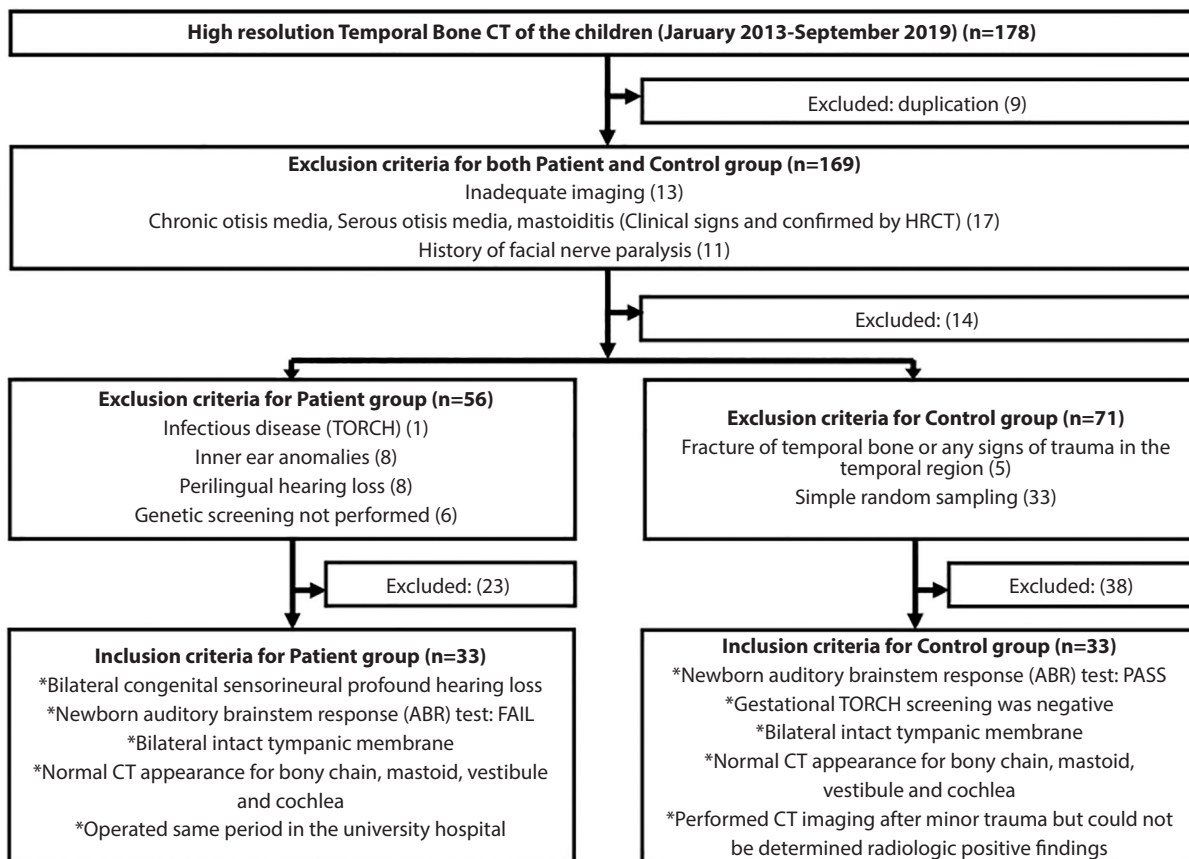


Figure 1. Study flowchart. The inclusion and exclusion criteria for the patient and control groups are summarized. All ears (external, middle, and inner ear) included in the study were intended to be completely radiologically normal.

was not possible to evaluate these three patients when blinded. The control group included patients who had undergone HRCT due to minor trauma but had no pathology. All the patients in the control group underwent hearing screening tests during the neonatal period, and all of them passed these tests. The hospital information system records of these patients were examined. In particular, patients whose physical examination results were normal and who had no record of hearing loss were selected. The control group was formed via selection from among 66 possible cases using the simple random sampling method during the same period. Sixty-six ears from 33 individuals were included in the control group.

Computed Tomography Imaging and PACS

All the CT scans were performed at our university hospital (GE Optima CT660; GE Healthcare, Milwaukee, Wisc., USA) by using a helical temporal bone protocol. All the CT scans were performed with the patient in the supine position without the gantry angle. The scanning range included the whole temporal bone. The CT image data were collected with a GE system equipped with a 512×512 matrix detector, with a slice thickness with 0.625 mm depth, and measured with an exposure value of 110 kV 250 mAs. The window width was 3,000 HU, and the window level was 500 HU. These raw data projection images were recorded and reconstructed with three-dimensional (3D) multiplanar reconstruction (3D-MPR) using HOROS, open-source imaging software for Mac OS X (a trademark of The HOROS project) to obtain the required planes. 3D-MPR was used to measure the length of the cochlea and its subparts.

Measurement Protocol

The target structure in our measurements was the outer wall of the cochlea (LW). The measurements were performed with the previously described cochlear view and followed the middle and apical turns^[10, 11]. Being the previously accepted landmark, the round window was

the starting point for the measurement^[26]. The cochlear view was defined as the x axis, and the y and z axes were set to follow this axis perpendicular to the cochlear aperture and modiolus^[26]. From the round window onward, we used 11-12 guide points, depending on where the apex ended (Figure 2). Each point on the curve was placed at a 90° angle. The Horos software drew the curve between the points automatically. Similar to previous studies, from the round window, the first 360° angle was accepted as the basal turn (BW), the second 360° angle was considered the middle turn (MW), and the remaining part was accepted as the apical turn (AW). We used additional points when the following two points did not fit the cochlear LW curve. We carefully chose every point from the most external coordinate possible to avoid partial volume effect and beam hardening artifacts (Figure 3). Controls were made for each measurement in all three axes so that the measured points correspond to the middle part of the height in the examined cochlea^[27]. Middle turn measurement was challenging owing to the angle between the basal and the middle turn that was approximately 14.90°. If the angle was too wide, it was difficult to follow the middle and apical turns with the x axis (cochlear view) established in the basal turn. Thus, a partial volume effect was seen in the upper basal wall of the basal turn and the inferior wall of the middle turn^[13, 23]. Additionally, it was difficult to decide where the lateral wall curve was located in these segments because the dense cortex line was not observed in the middle turn outer wall.

The measurement was difficult at the apex level, especially at the endpoint (Figure 4). The height and width of the cochlea decreased as it moved from the round window to the apex^[6, 7, 13, 28]. The apex endpoint had a small volume and shape; therefore, it was difficult to follow the apex curve with in-vivo imaging. In order to overcome these challenges, the coordinates marked in the axes (y and z) perpendicular to the cochlear view were checked and repositioned when necessary.

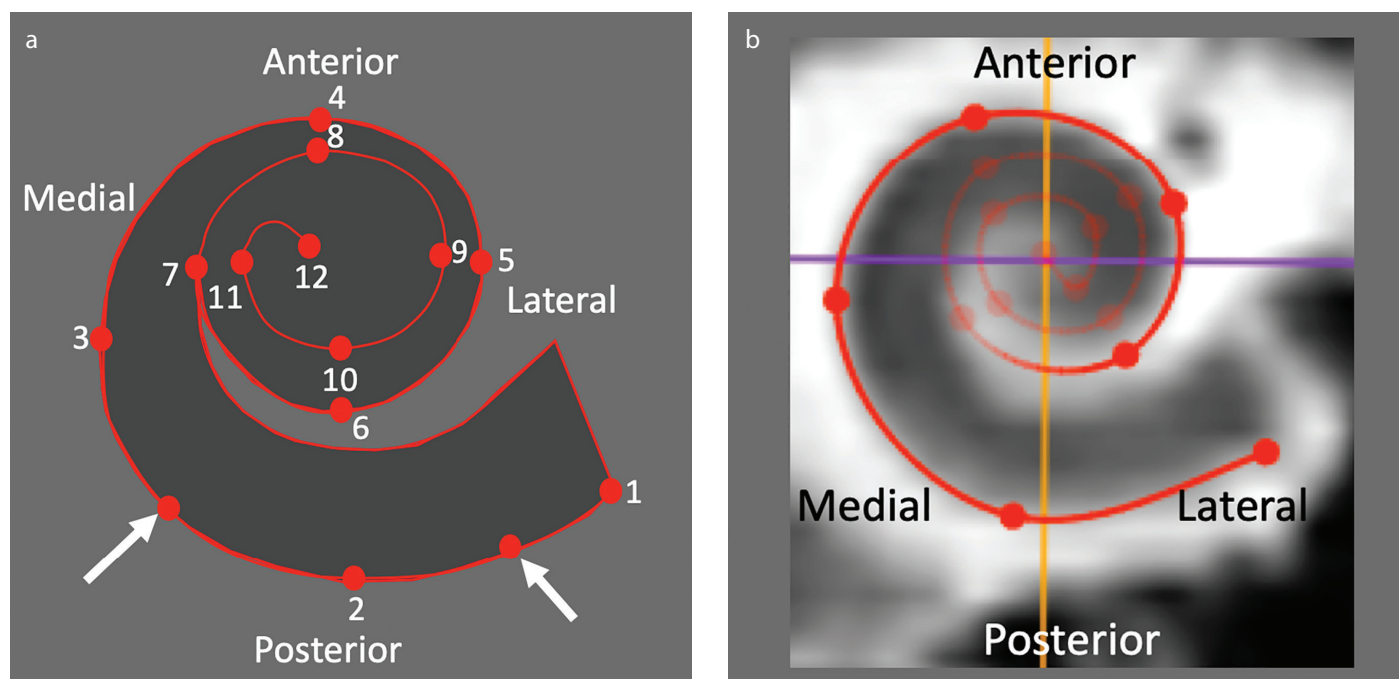


Figure 2. a, b. a) Scheme of the Cochlea. b) Cochlear view. The reference points for measurements (left cochlea). Following points for measurement; the first point was round window (1) and subsequent points (2-11) were placed with 90 degrees angle. The most prominent point in the midline of each lateral wall segment (with 90° angle range). The hook and endpoint (12). The white arrows indicate where the most additional points were used for curve correction.

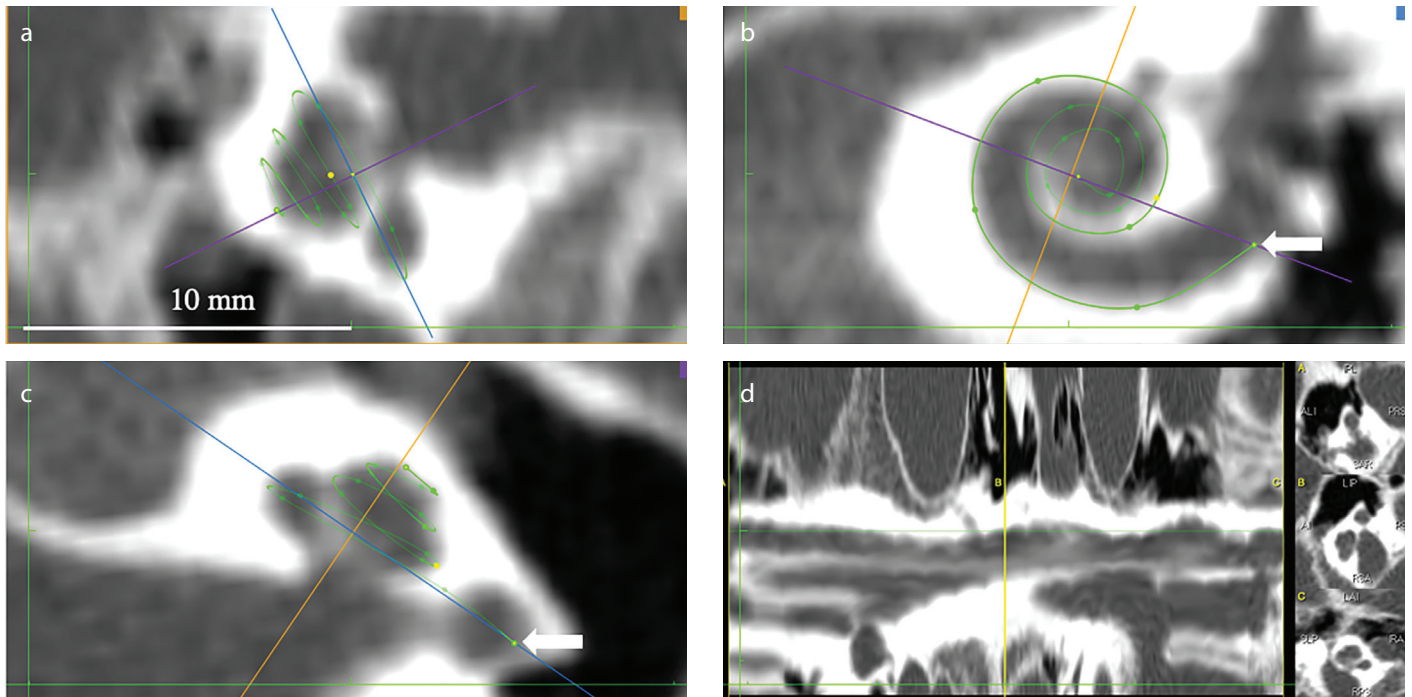


Figure 3. a-d. The measurement screen at the starting point; a) and c) show the y and z axes perpendicular to the cochlear aperture and modiolus, and B presents the cochlear view. The white arrows in b) and c) indicate the starting point. d) presents the curved 3D-MPR image and the whole cochlea.

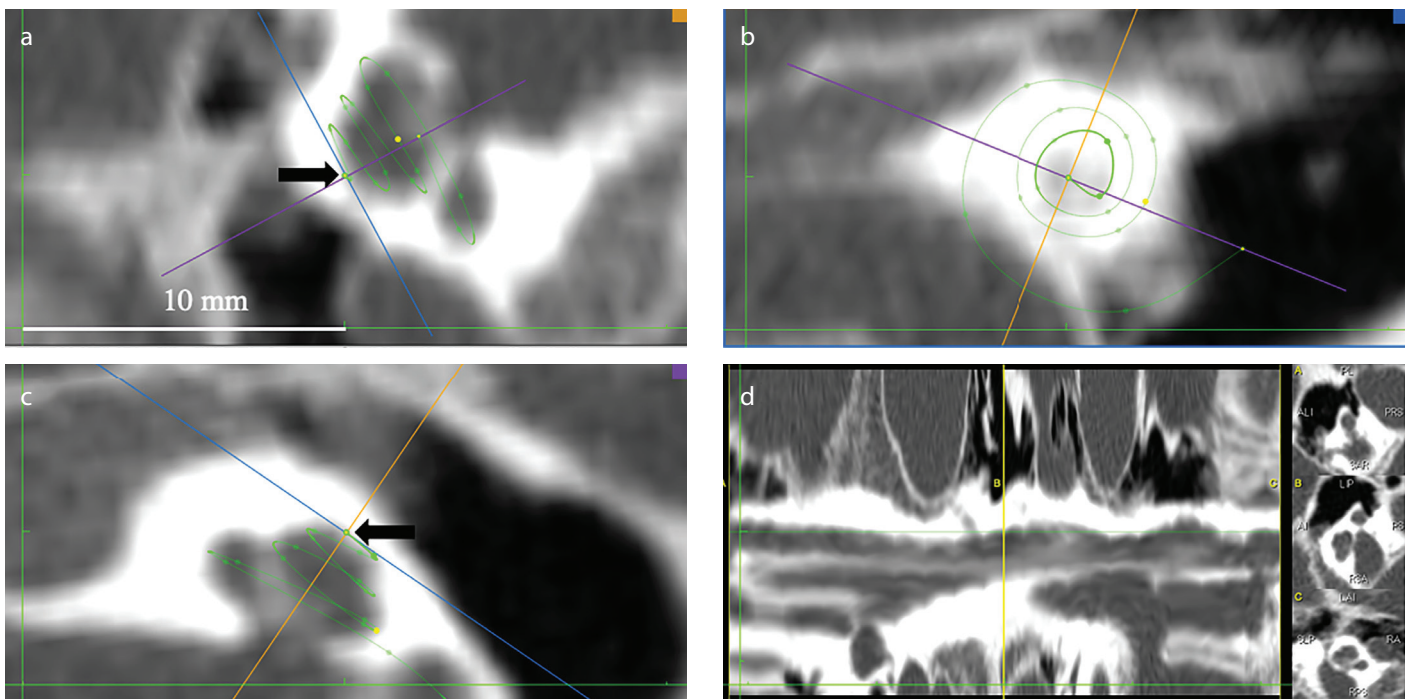


Figure 4. a-d. The measurement screen at the endpoint; a) and c) show the y and z axes, and b) presents the apical endpoint of the measurement in the x axis. The black arrows in a) and c) indicate the endpoint of the measurement in the apical turn in the y and z axes, respectively. D presents the curved 3D-MPR image and the whole cochlea.

In order to prevent prejudice, data of patients from both the groups were randomly entered into an MS Excel file. The data were delivered to an experienced radiologist for the necessary measurements.

Trial measurements were performed once on all ears before the study. Then, at different times, all the measurements in the patient and control groups were repeated three times.

Statistical Analysis

The distribution of the data was assessed using the Kolmogorov-Smirnov test. In order to evaluate intra-rater reliability, intra-class correlation coefficient (ICC) was used; further, 95% confident intervals were calculated based on a mean-rating (k=3), absolute-agreement, 2-way mixed-effects model. ICC values <0.50 indicate poor reliability, values of 0.50-0.75 indicate moderate reliability, values of 0.75-0.90

indicate good reliability, and values >0.90 show excellent reliability. Independent sample t-test was used to compare the variables of the patient and control groups as well as to make sex-based comparisons within each group. In each subgroup, right and left-ear comparisons were performed using a paired sample t-test. Pearson's correlation was performed to compare the lengths of the subparts and the whole cochlea. Regression analysis was performed when the correlation was high. The ROC curve analysis was used to determine the cut-off values for LW, BW, MW and AW between CSNHL patients and normal group participants. $p < 0.05$ indicated statistical significance. The data were analyzed using The Statistical Package for the Social Sciences (SPSS) 22.0 for Mac OS X (IBM Corp.; Armonk, NY, USA).

Determination of Sample Size

Power analysis was performed using G * Power 3.1.9.3 for Mac Os X (<http://www.gpower.hhu.de/>). To our knowledge, no research has been previously conducted on the present subject; therefore, LW-related descriptive statistical information was unavailable, especially regarding the patient group. Thus, instead of prior power analysis, the appropriate sample size was determined via interim evaluations. When the number of subjects in the groups reached 15, a power analysis was performed. The results showed that the difference was significant when the prior power was 80%, first-type error probability was 5%, and effect size was 2.5 ± 0.8 . However, the study was continued, and power analysis performed again. When the standardized effect size was taken as $d = 1.98$, $\alpha = 5\%$, the retrospective power value was 99.99%.

RESULTS

Demographic Characteristics

The study and control groups were comparable in terms of age (Table 1), and all variables for both ears in each group showed normal distribution in the Kolmogorov-Smirnov test (Table 2). In the CSNHL group, the mean length of lateral wall was significantly shorter for both the entire and subparts of cochlea than the control group (Table 3).

Measurement Validity and Spiral Equations

The intra-rater reliability of the method was 0.878 (CI 95%, 0.841–0.908, $p < 0.001$). The test-retest reliability of our method ranges from “good” to “excellent”.

Previous studies suggested different spiral equations to estimate cochlea length.^[2,29] Therefore, Pearson's correlation test was used for the patient and control groups in order to evaluate the compatibility between the measurements of the subparts and the LW. This analysis included a comprehensive assessment of all the ears; the results are summarized in Table 4.

Regression analysis was performed to identify the subparts that could adequately predict the whole cochlear LW length with high correlation. In the control and patient group, the correlation between LW and the BW was good ($R^2 = 0.553$, $p < 0.001$ – $R^2 = 0.571$, $p < 0.001$). The correlation equation summarized in figure 5. The correlation between LW and the MW was good for controls and moderate for patients ($R^2 = 0.642$, $p < 0.001$ – $R^2 = 0.499$, $p = 0.003$). In the control group, the correlation between LW and the AW was good

Table 1. Descriptive statistics by age

	n	Mean age (months)	SD	Range (min–max)
CSNHL*	33	26.91	15.88	6-61
Female**	17	24.88	15.47	8-61
Male**	16	29.06	16.53	6-57
Control*	33	37.39	21.10	5-87
Female***	15	33.13	13.44	5-52
Male***	18	40.94	25.69	13-87

CSNHL: Congenital sensorineural hearing loss. $p = 0.43^*$, $p = 0.46^{**}$, $p = 0.68$

Table 2. Descriptive statistics for the LW of all the ears as per patient sex (mm)

	n	Mean	SD	CI-95%	K-S test
CSNHL	33	39.71	1.32	39.25-40.18	0.186
Female*	17	39.60	1.37	38.89-40.31	0.200
Male*	16	39.84	1.29	39.14-40.53	0.056
Control	33	42.09	1.17	41.67-42.51	0.161
Female**	15	41.81	1.12	41.18-42.43	0.200
Male**	18	42.32	1.20	41.73-42.92	0.200

CSNHL: Congenital sensorineural hearing loss; CI-95%: Confidence interval, K-S test: Kolmogorov–Smirnov test. $p = 0.617^*$, $p = 0.214^{**}$

Table 4. The results of Pearson's correlation analysis of the lateral wall subpart measurements

	SNHL	r	p
BW	CSNHL	0.755	<0.001
	Control	0.744	<0.001
MW	CSNHL	0.499	0.003
	Control	0.642	<0.001
AW	CSNHL	0.209	0.244
	Control	0.563	0.001

CSNHL: Congenital sensorineural hearing loss; BW: Basal turn lateral wall length; MW: Middle turn lateral wall length; AW: Apical turn lateral wall length.

Table 3. Cochlea and subpart measurements performed in the CSNHL and control groups (mm)

	SNHL	n	Mean	SD	CI-95%	p
LW	CSNHL	33	39.71	1.32	39.25-40.18	<0.001
	Control	33	42.09	1.17	41.67-42.51	
BW	CSNHL	33	21.66	1.01	21.30-22.02	<0.001
	Control	33	22.57	0.68	22.32-22.81	
MW	CSNHL	33	11.58	0.69	11.34-11.83	<0.001
	Control	33	12.39	0.46	12.23-12.56	
AW	CSNHL	33	6.45	0.92	6.12-6.77	0.001
	Control	33	7.12	0.60	6.89-7.35	

LW: Cochlea lateral wall length; BW: Basal turn lateral wall length; MW: Middle turn lateral wall length; AW: Apical turn lateral wall length; SNHL: Sensorineural hearing loss; CSNHL: Congenital sensorineural hearing loss; CI-95%: Confidence interval.

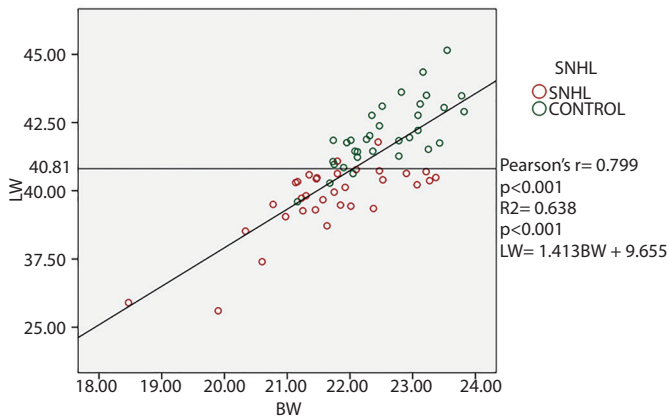
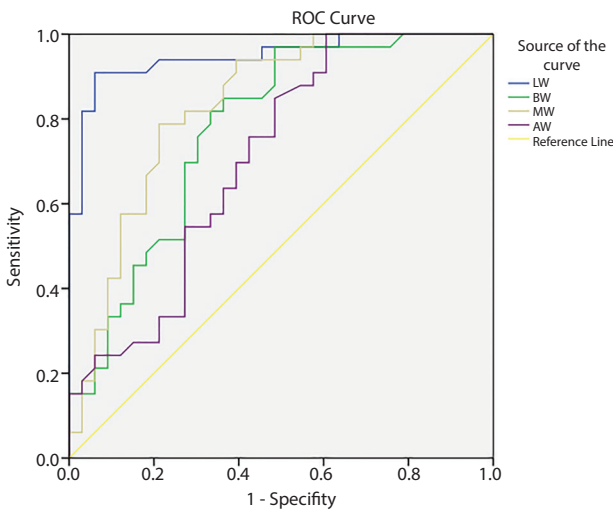


Figure 5. The regression equation of the whole LW and BW.



Diagonal segments are produced by ties.

Figure 6. ROC curves of the LW, BW, MW, and AW. The areas under the curves (AUCs) for the LW, BW, MW, and AW are 0.948, 0.776, 0.831, and 0.707, respectively.

Table 6. LW and OC length measurements (mm)

Authors/Year	Target Structure	Method	N (Ears)	Mean (SD)	Minimum-Maximum
Hardy, 1938	OC	Histology	68	31.57 (2.3)	25.26-35.46
Kawano et al., 1996	OC	Histology	8	35.58 (1.41)	34.15-37.9
Kawano et al., 1996	LW	Histology	8	40.81 (1.97)	37.93-43.81
Stakhovskaya et al., 2007	OC	Histology	9	33.13 (2.11)	30.5-36.87
Erixon et al., 2009	LW	Plastic molds	58	42 (1.96)	38.6-45.6
Erixon & Rask-Andersen 2013	LW	Plastic molds	51	41.2 (1.86)	37.6-44.9
Wüffel et al., 2014	LW	CBCT 3D-MPR	436	37.9 (1.98)	30.8-43.2
Meng et al., 2016	LW	HRCT 3D-MPR	310	35.8 (2.00)	30.7-42.2
Pietsch et al., 2017	LW	µCT-Plastic molds	138	40.9 (2.00)	36-46
Current Study (All ears)	LW	HRCT 3D-MPR	129	40.9 (1.72)	35.60-45.15
Current Study (CSNHL)	LW	HRCT 3D-MPR	63	39.71 (1.32)	35.60-41.79
Current Study (Control)	LW	HRCT 3D-MPR	66	42.09 (1.17)	39.60-45.15

(R2=0.563, p=0.001), unlike the correlation was weak in the patient group (R2=0.209, p=0.244).

ROC

Table 5 summarizes the results of the ROC analysis for the LW, MW, and AW. The optimal cut-off value was 40.81 mm for the LW, differentiating the CSNHL patient group from the control group; the analysis had a sensitivity of 0.909 (3/33) and a specificity of 0.939 (2/33) (Figure 6).

DISCUSSION

In the current study, we evaluated CSNHL patients who were non-syndromic with a normal-appearing cochlea on HRCT according to the Sennaroglu classification [25]. We set out with the hypothesis that CSNHL patients cochleae might have dimensional differences although their anatomy were normal. The fact that the etiology of deafness can alter cochlear configuration should be remembered [17, 18, 31]. Further research on this topic may clarify this issue.

Cochlear Length

The most important result of this study was that the LW length was significantly different between the CSNHL and control groups. The findings for the control group in the current study were in agreement with those reported by Erixon et al. in 2009 [4] and 2013 [5], Pietsch et al. [7], and Kawano et al. [12]. In the current study the findings for

Table 5. Receiver operating characteristic analyses results of the whole cochlea and its subparts

Cochlear part	AUC	Youden index	Cut-off value (mm)	Sens	Spec	Acc
LW	0.948 (95% CI: 0.895–1.000)	0.86	40.81	0.91	0.94	0.90
BW	0.776 (95% CI: 0.501–0.854)	0.46	22.03	0.76	0.70	0.55
MW	0.831 (95% CI: 0.730–0.931)	0.58	12.14	0.79	0.79	0.66
AW	0.707 (95% CI: 0.581–0.833)	0.37	6.89	0.64	0.73	0.41

AUC: area under the curve; CI: confidence interval; Sens: sensitivity; Spec: specificity; Acc: Accuracy; LW: Cochlea lateral wall length; BW: Basal turn lateral wall length; MW: Middle turn lateral wall length; AW: Apical turn lateral wall length.

the basal and middle turns in the control group were similar with the literature [4, 5, 7, 12]. The apical turn measurements in our control group showed a difference of 1 mm as compared to the results reported by Erixon et al. because the decision on the endpoint was different [4, 5] (Table 6).

Meng et al. [13] and Würfel et al. [14] used 3D MPR, similar to that in the current study. However, our study was methodologically different from these researches. The results of these two studies are different from our findings. As mentioned in the Methods section, we measured the most prominent point in the midline of each LW segment. It is challenging to detect this point with imaging; an area of intermediate density appears on imaging, owing to the partial volume effect and the beam-hardening artifact between the fluid-filled cochlea and the outer wall with a thick cortex [27]. Previous researchers may have placed the reference points in areas of intermediate density where the partial volume and beam hardening were intense [13, 14, 30]. These two studies measured the AW and found it shorter than that reported in the literature [4-7, 12]. This study was performed by using fully hyperdense reference points that were located more laterally than that in previous studies to ensure minimal partial volume effect. In this process, we ensured that there was no remaining pixel of hypodense and intermediate densities out of the area of the curve we drew. Different results may not be explained by the method alone. The cochlea size may be influenced by variables, such as age, sex, ethnicity, and geography, thus affecting the results [31-33]. However, irrespective of the radiological method used, the medial-upper wall of the basal turn and the lateral-lower wall of the middle turn are adjacent and exert additional partial volume effect. A review of previous studies shows that the different measurement techniques differ in their results. Therefore, it would be useful to determine references not only for the starting point but also other points of measurement as well as develop a more practical method for identifying the optimal endpoint.

Cochlear Microanatomy

This study found that both the whole cochlea and its subparts were shorter in the patient group than in the controls. This raises the following question: in which subpart was this difference more pronounced? To answer this question, the ratio of the length of LW to the length of BW, MW, and AW were calculated; these ratios were 54.54% and 53.62% for the BW, 29.16% and 29.43% for the MW, and 16.24% and 16.91% for the AW in the patient and control groups, respectively. The ratio of mean length values to each other in the patient and control groups were 95.96% for BW, 93.46% for MW, and 90.58% for AW. The cochlea of the CSNHL group was shorter than that of the control group; however, this difference was mostly and relatively due to the apical and middle turn. The mean length of the basal turn was relatively preserved in the study group compared to that of the other turns.

Patient-specific cochlear implant selection before surgery affects the success of CI surgery [19, 34]. If the electrode is chosen as per the cochlea size, the surgeon will get a chance to tailor the insertion depth as needed [21]. Moreover, this would facilitate post-operative fitting of the speech processor to match the patient's tonotopy [8, 9, 21, 22]. Deep implantation is a preferred and favorable method for successful CI [24]. However, unsuitable long electrode selection with the patient's

cochlear anatomy may lead to trauma during surgery. [21]. The use of a short cochlear implant may not produce the targeted hearing results for the big cochlea [8, 9, 20-23].

Estimated Cochlear Length

Previous studies by Würfel et al. were based on either reformatted images, such as those in studies by Purcell et al. or calculations using a mathematical formula involving the "A" value defined by Escudé et al. [2, 17, 22, 35]. The value of "A" refers to the line drawn from the midline of the round window in the cochlear view to the most prominent point in the basal turn. This point is 180° degrees away from the starting point (Figure 3). Subsequent studies have shown that this value alone is a good but inadequate indicator. These propositions are practical for clinical use and a good indicator of the basal turn [4, 5, 29]. However, the middle turn and full cochlear length are inadequate in estimation because cochlear anatomy shows wide variations, especially in the middle and apical turns [4-7]. Our findings also support these hypotheses. Our correlation analysis revealed that the whole cochlear length had a medium correlation with the lengths of middle and apical turns and a good correlation with the basal turn. Therefore, we performed a linear regression analysis. The outcome shows that determining the basal turn length can provide information about the whole length of the cochlea. Preoperative measurements performed using 3D reconstructed images can be very useful for this patient group.

Limitations

The main limitation of this study is that the measurements were performed by a single observer. However, the reproducibility was good for intra-rater ICC.

The sample size appears to be another limitation; however, we do not think that repeating the study in the same population will contribute to the literature because the sample size is sufficient and the results have high sensitivity and specificity values in the ROC analysis. However, repeating the study in different populations would be valuable because of the opportunity of studying the effect of different variables on the results, such as ethnicity, geographical location, sex, materials used, and method employed.

CONCLUSION

Our results showed that the lengths of the whole cochlea and that of each subpart were significantly shorter in CSNHL patients than in healthy controls. There may be microanatomic differences in the cochlea of those with normal hearing and those with CSNHL. We believe that repeating this study in different populations will provide useful data; further, determination of the cochlear length before CI will increase the success rate.

Informed Consent: This study was approved by the Istanbul Medeniyet University, Göztepe Training and Research Hospital Ethics Committee for Clinical Studies (17 May 2018, 2018/0177).

Informed Consent: Informed consent was waived by Ethics Committee.

Peer-review: Externally peer-reviewed.

Author Contributions: Concept – M.B.E., B.A., M.T.K.; Design – M.B.E., B.A.; Supervision – B.A., M.T.K.; Resource – M.B.E., M.T.K.; Materials – M.B.E., B.A., M.T.K.; Data Collection and/or Processing – M.B.E., B.A., M.T.K.; Analysis and/or Inter-

pretation - M.B.E., B.A.; Literature Search - M.B.E., B.A.; Writing - M.B.E., B.A., M.T.K.; Critical Reviews - M.B.E., B.A., M.T.K.

Acknowledgements: The authors would like to thank Christine Margaret Calvert for proof-reading and Prof. Handan Ankarali, Ph.D. to help for statistical evaluation.

Conflict of Interest: The authors have no conflict of interest to declare.

Financial Disclosure: The authors declare that this study has received no financial support.

REFERENCES

- Koch RW, Ladak HM, Elfarnawany M, Agrawal SK. Measuring Cochlear Duct Length - a historical analysis of methods and results. *J Otolaryngol Head Neck Surg* 2017; 46: 19.
- Escudé B, James C, Deguine O, Cochard N, Eter E, Fraysse B. The size of the cochlea and predictions of insertion depth angles for cochlear implant electrodes. *Audiol Neurootol* 2006; 11 Suppl 1: 27-33.
- Koch RW, Elfarnawany M, Zhu N, Ladak HM, Agrawal SK. Evaluation of Cochlear Duct Length Computations Using Synchrotron Radiation Phase-Contrast Imaging. *Otol Neurotol* 2017; 38: e92-9.
- Erixon E, Högstorp H, Wadin K, Rask-Andersen H. Variational anatomy of the human cochlea: implications for cochlear implantation. *Otol Neurotol* 2009; 30: 14-22.
- Erixon E, Rask-Andersen H. How to predict cochlear length before cochlear implantation surgery. *Acta Otolaryngol* 2013; 133: 1258-65.
- Avci E, Nauwelaers T, Lenarz T, Hamacher V, Kral A. Variations in micro-anatomy of the human cochlea. *J Comp Neurol* 2014; 522: 3245-61.
- Pietsch M, Aguirre Dávila L, Erfurt P, Avci E, Lenarz T, Kral A. Spiral Form of the Human Cochlea Results from Spatial Constraints. *Sci Rep* 2017; 7: 7500.
- Sridhar D, Stakhovskaya O, Leake PA. A frequency-position function for the human cochlear spiral ganglion. *Audiol Neurootol* 2006; 11 Suppl 1: 16-20.
- Stakhovskaya O, Sridhar D, Bonham BH, Leake PA. Frequency map for the human cochlear spiral ganglion: implications for cochlear implants. *J Assoc Res Otolaryngol* 2007; 8: 220-33.
- Marsh MA, Xu J, Blamey PJ, Whitford LA, Xu SA, Silverman JM, et al. Radiologic evaluation of multichannel intracochlear implant insertion depth. *Am J Otol* 1993; 14: 386-91.
- Xu J, Xu SA, Cohen LT, Clark GM. Cochlear view: postoperative radiography for cochlear implantation. *Am J Otol* 2000; 21: 49-56.
- Kawano A, Seldon HL, Clark GM. Computer-aided three-dimensional reconstruction in human cochlear maps: measurement of the lengths of organ of Corti, outer wall, inner wall, and Rosenthal's canal. *Ann Otol Rhinol Laryngol* 1996; 105: 701-9.
- Meng J, Li S, Zhang F, Li Q, Qin Z. Cochlear Size and Shape Variability and Implications in Cochlear Implantation Surgery. *Otol Neurotol* 2016; 37: 1307-13.
- Würfel W, Lanfermann H, Lenarz T, Majdani O. Cochlear length determination using Cone Beam Computed Tomography in a clinical setting. *Hear Res* 2014; 316: 65-72.
- Würfel W, Burke WF, Lenarz T, Kraemer R. Cochlear length determination in temporal bone specimens using histological serial Micro grinding imaging, micro computed tomography and flat-panel volumetric computed tomography. *Otolaryngology Online Journal* 2015; 5. Available from: <https://www.alliedacademies.org/articles/cochlear-length-determination-in-temporal-bone-specimens-using-histological-serial-micro-grinding-imaging-micro-computed-tomography-and-flatpanel-volumetric-computed-tomography.pdf>
- Sakellarios AI, Tachos NS, Rigas G, Bibas T, Ni G, Bohnke F, et al. A validated methodology for the 3D reconstruction of cochlea geometries using human microCT images. *Meas Sci Technol* 2017; 10.1088/1361-6501/aa5f18.
- Purcell DD, Fischbein N, Lalwani AK. Identification of previously "undetectable" abnormalities of the bony labyrinth with computed tomography measurement. *Laryngoscope* 2003; 113: 1908-11.
- Shim HJ, Shin JE, Chung JW, Lee KS. Inner ear anomalies in cochlear implantees: importance of radiologic measurements in the classification. *Otol Neurotol* 2006; 27: 831-7.
- Schurzig D, Timm ME, Batsoulis C, Salcher R, Sieber D, Jolly C, et al. A Novel Method for Clinical Cochlear Duct Length Estimation toward Patient-Specific Cochlear Implant Selection. *OTO Open* 2018; 2: 2473974X18800238.
- Dhanasingh A, Jolly C. An overview of cochlear implant electrode array designs. *Hear Res* 2017; 356: 93-103.
- Dhanasingh A. Cochlear duct length along the outer wall vs organ of corti: Which one is relevant for the electrode array length selection and frequency mapping using Greenwood function? *World J Otorhinolaryngol Head Neck Surg* 2018; 5: 117-21.
- Mistik P, Jolly C. Optimal electrode length to match patient specific cochlear anatomy. *Eur Ann Otorhinolaryngol Head Neck Dis* 2016; 133 Suppl 1: S68-71.
- De Seta D, Torres R, Russo FY, Ferrary E, Kazmitcheff G, Heymann D, et al. Damage to inner ear structure during cochlear implantation: Correlation between insertion force and radio-histological findings in temporal bone specimens. *Hear Res* 2017; 344: 90-7.
- Nayak G, Panda NK, Banumathy N, Munjal S, Khandelwal N, Saxena A. Deeper insertion of electrode array result in better rehabilitation outcomes - do we have evidence? *Int J Pediatr Otorhinolaryngol* 2016; 82: 47-53.
- Sennaroglu L, Bajin MD. Classification and current management of inner ear malformations. *Balkan Med J* 2017; 34: 397-411.
- Verbist BM, Skinner MW, Cohen LT, Leake PA, James C, Boex C, et al. Consensus panel on a cochlear coordinate system applicable in histologic, physiologic, and radiologic studies of the human cochlea. *Otol Neurotol* 2010; 31: 722-30.
- Bushberg JT, Seibert JA, Leidholdt EM, Boone JM, Goldschmidt EJ. *The Essential Physics of Medical Imaging*. Philadelphia: Lippincott Williams & Wilkins press; 2012. p.368-77.
- Demarcy T, Vandersteen C, Guevara N, Raffaelli C, Gnansia D, Ayache N, et al. Automated analysis of human cochlea shape variability from segmented μ CT images. *Comput Med Imaging Graph* 2017; 59: 1-12.
- Alexiades G, Dhanasingh A, Jolly C. Method to estimate the complete and two-turn cochlear duct length. *Otol Neurotol* 2015; 36: 904-7.
- Lexow GJ, Kluge M, Gellrich NC, Lenarz T, Majdani O, Rau TS. On the accuracy of cochlear duct length measurement in computed tomographic images. *Eur Arch Otorhinolaryngol* 2018; 275: 1077-85.
- Pelliccia P, Venail F, Bonafé A, Makeieff M, Iannetti G, Bartolomeo M, et al. Cochlea size variability and implications in clinical practice. *Acta Otorhinolaryngol Ital* 2014; 34: 42-9.
- Thong JF, Low D, Tham A, Liew C, Tan TY, Yuen HW. Cochlear duct length-one size fits all? *Am J Otolaryngol* 2017; 38: 218-21.
- Grover M, Sharma S, Singh SN, Kataria T, Lakhawat RS, Sharma MP. Measuring cochlear duct length in Asian population: worth giving a thought. *Eur Arch Otorhinolaryngol* 2018; 275: 725-8.
- Timm ME, Majdani O, Weller T, Windeler M, Lenarz T, Büchner A, et al. Patient specific selection of lateral wall cochlear implant electrodes based on anatomical indication ranges. *PLoS One* 2018; 13: e0206435.
- Deep NL, Howard BE, Holbert SO, Hoxworth JM, Barrs DM. Measurement of cochlear length using the 'A' value for cochlea basal diameter: A feasibility study. *Cochlear Implants Int* 2017; 18: 226-9.